*Proc. Natl. Acad. Sci. USA*
Vol. 82, pp. 4110–4114, June 1985
Biophysics

# Interactions between acidic proteins and crystals: Stereochemical requirements in biomineralization

**(calcification/mollusk shells/organic matrix/crystal orientation/calcite)**

L. ADDADI* AND S. WEINER†

Departments of *Structural Chemistry and †Isotopes, Weizmann Institute of Science, Rehovot, 76100 Israel

*Communicated by H. A. Lowenstam, March 25, 1985*

ABSTRACT **Acidic matrix macromolecules are intimately involved in biological crystal growth. *In vitro* experiments, in which crystals of calcium dicarboxylate salts were grown in the presence of aspartic acid-rich proteins, revealed a stereochemical property common to all the interacting faces. Calcite crystals are nucleated on stereochemically analogous faces when proteins are adsorbed onto a rigid substrate. The importance of this property in biomineralization is discussed.**

Biologically formed crystals are an integral part of many organisms. Their presence in the skeletons of invertebrates and vertebrates is particularly widespread. The crystals often are all of uniform size, have oriented crystallographic axes, and adopt sizes and shapes ("crystal habits") quite different from those found in their nonbiological counterparts. These properties indicate that the crystals form under well-controlled conditions. A common mode of crystal growth in these tissues is through the initial formation of a structural framework (the "organic matrix") in which the crystals subsequently grow (1). The regulation of crystal growth is partly accomplished by an array of matrix macromolecules, many of which are synthesized by specific cells for this purpose (2–4). A subset of the matrix macromolecules are closely associated with the mineral phase and hence are thought to regulate crystal growth by some as yet unknown mechanisms (2). These macromolecules are characteristically acidic in nature (2–5).

One widely used approach for studying the functions of these acidic macromolecules is to examine in various ways their effect on crystal growth *in vitro*. The kinetics of crystal growth have been measured in the presence of different matrix macromolecules under a variety of conditions (6–9). Combinations of matrix components have been used to detect a collaborative effect (10), and the ability of demineralized matrix to induce crystal nucleation has been examined (11, 12). In this study, we used a different *in vitro* approach. We examined the manner in which acidic matrix macromolecules interact with different structured surfaces of various crystals. Our objective was to understand the principles that govern these interactions and to gain insight into the mechanisms by which these matrix constituents regulate crystal growth *in vivo*. We report here a particular stereochemical property of the crystal surfaces we examined that appears to be an essential requirement for interaction to occur with one of the major groups of matrix constituents, the acidic proteins. These same proteins, once adsorbed on a rigid support, act as nucleators of calcite from the specific crystal plane that the stereochemical rules indicate is the best plane of interaction.

The experimental tool we used to investigate these interactions was adapted from recently reported mechanistic studies of the effect of "tailor-made" low molecular weight additives on the growth of organic crystals (13, 14). These studies showed that stereoselective adsorption of an additive onto a specific crystal face results in a drastic decrease in its growth rate relative to that of unaffected faces. Since the crystal morphology is determined by the relative growth rate of the slowest-growing faces, the interaction of the additive with the crystal affects the overall morphology (Scheme 1).

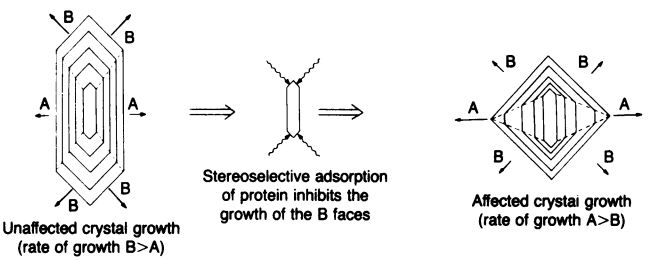


Scheme 1

Analysis of morphological changes is, therefore, a means of pinpointing the specific crystal faces that adsorb the additive (thus increasing in relative area) and thereby of studying the nature of the interactions between the two. We used different matrix macromolecules extracted from mollusk shells as the additives and crystals of various calcium dicarboxylates, as well as calcite, as the substrates.

The acidic organic matrix proteins were obtained from either the calcitic or the aragonitic layers of the bivalve *Mytilus californianus*. Two different classes of proteins were extracted and purified as described (15). One fraction is composed of the aspartic acid-rich proteins (amino acid composition: Asx, 32%; Ser, 10%; Glx, 17%; Gly, 7%), possibly associated with small amounts of polysaccharide, and the second fraction contains serine-rich proteins that are associated with relatively large amounts of polysaccharides (amino acid composition: Asx, 7%; Ser, 25%; Glx, 8%; Gly, 19%). Constituents of both fractions bind $Ca^{2+}$ and upon doing so undergo conformational changes. The aspartic acid-rich proteins adopt the $\beta$-sheet conformation (unpublished observation). The crystals grown in the presence of these matrix molecules were calcium salts of dicarboxylic acids [calcium fumarate trihydrate (17), calcium malonate dihydrate (18), calcium tartrate tetrahydrate (19), and calcium maleate monohydrate‡] and the calcium carbonate polymorph calcite.

## MATERIALS AND METHODS

**Crystal Growth Conditions.** The optimal conditions for crystallizing the pure compounds from water at pH 7.0 were determined, so that the crystals formed were homogeneous

The publication costs of this article were defrayed in part by page charge payment. This article must therefore be hereby marked "*advertisement*" in accordance with 18 U.S.C. §1734 solely to indicate this fact.

‡The structure of this polymorph was determined by F. Frolow, Structural Chemistry Dept., Weizmann Institute (personal communication).

and reproducible with respect to morphology. The habit of typical crystals and the relative areas of the developed faces were measured on a Siemens x-ray diffractometer by use of standard techniques (14, 20). The effect of matrix macromolecules on crystal morphology was examined by adding them in appropriate amounts (stock solution of 300 μg/ml in 5 mM $CaCl_2$ at pH 7) to filtered supersaturated calcium dicarboxylate solutions (1 ml) prior to the onset of crystallization. The morphology of crystals formed in the presence of protein (affected crystals) was compared to that of crystals grown in parallel without protein (control crystals). Crystal growth of calcium dicarboxylate salts at room temperature occurred within 24 hr for control solutions and within 1–2 weeks in the presence of protein.

Solutions were prepared as follows. *Calcium malonate dihydrate*: 50 mg of malonic acid and 50 mg of $CaCl_2 \cdot 2H_2O$ were dissolved in 7 ml of double-distilled water. The solution was titrated to pH 7.3 with 1 M NaOH and then filtered through glass wool. *Calcium fumarate trihydrate*: 165 mg of fumaric acid and 110 mg of $Ca(OH)_2$ were suspended in 10 ml of double-distilled water, acidified with 1 M HCl until all the compound dissolved (pH ≈ 2.5), and then titrated to pH 7.0 with 1 M NaOH. *Calcium maleate monohydrate*: 450 mg of maleic acid and 280 mg of $Ca(OH)_2$ were added to 10 ml of double-distilled water, acidified with 1 M HCl until all the compound dissolved, and then titrated to pH 7.0 with 1 M NaOH. *Calcium tartrate tetrahydrate*: 5.0 ml of a solution of 57 mg of sodium potassium tartrate were mixed with 5.0 ml of a solution containing 40 mg of $CaCl_2 \cdot 2H_2O$ at pH 6.7. *Calcite*: crystallization was induced by slow diffusion of ammonium carbonate vapor into 1 ml of 7.5 mM $CaCl_2$ (pH 7.0) in a closed dessicator for 1–2 days.

**Immunofluorescence Labeling.** Crystals were incubated for 2 hr in rabbit serum diluted 10-fold with 5 mM $CaCl_2$ containing antibodies raised against an HPLC-purified fraction of aspartic acid-rich proteins from the nacreous layer of *M. californianus*. The crystals were washed with the $CaCl_2$ solution, incubated for 2 hr with fluorescein isothiocyanate (FITC)-labeled goat antibodies against rabbit immunoglobulins (50 μg/ml in 5 mM $CaCl_2$), and rewashed.

## RESULTS

**Calcium Malonate/Aspartic Acid-Rich Protein System.** The calcium malonate crystals grown in the absence of protein are prismatic and elongated along the *c* axis. The predominant faces are {100}, {110}, and {010} (Fig. 1*A*). The crystals grown in the presence of protein are elongated along the *b* axis and the predominant faces are {101}, {10$\bar{1}$}, and {110} (Fig. 1*B*). The protein concentrations were calculated from the yields of amino acids upon hydrolysis and corresponded to 0.5–1.0 μg of protein/ml. Assuming an average molecular weight of 10,000 (15), this corresponds to a 10–100 nM protein solution. This protein concentration results in the maximal effect on the crystals. At lower protein concentrations (0.1–0.5 μg of protein/ml), the morphological change is more limited and proportional to the amount of protein in solution. An analysis of the crystal morphologies shows that acidic proteins specifically influenced the growth of the {101} and {10$\bar{1}$} faces, which developed at the expense of the {100}, {210}, and {001} faces. The characteristic feature of the {101} and {10$\bar{1}$} faces (Fig. 2) is the carboxylate orientation of the malonate molecules with respect to calcium. Two sets of malonate molecules (18), related by translation along the *b* axis, have the carboxylate groups emerging perpendicular to the face and complexing the calcium ions in either of the two repeating motifs shown in Scheme 2 *A* and *B*. Examination of all the other faces of the malonate crystals unaffected by

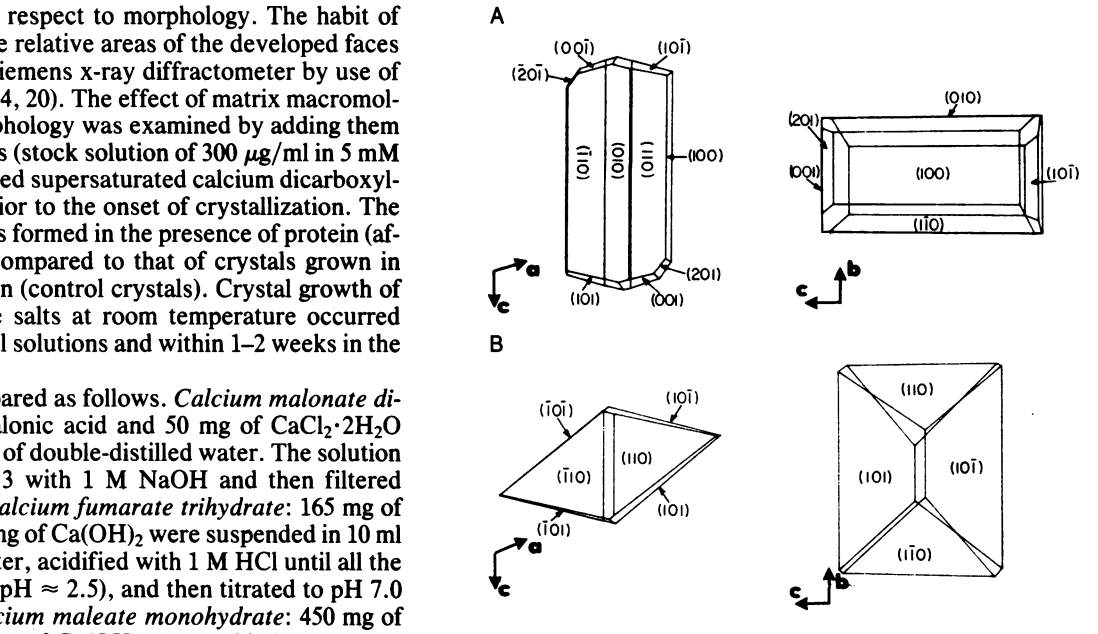


FIG. 1. Morphology of typical crystals of calcium malonate dihydrate in two different projections. (*A*) Pure calcium malonate. (*B*) Calcium malonate grown in the presence of 0.5 μg of protein/ml (affected).

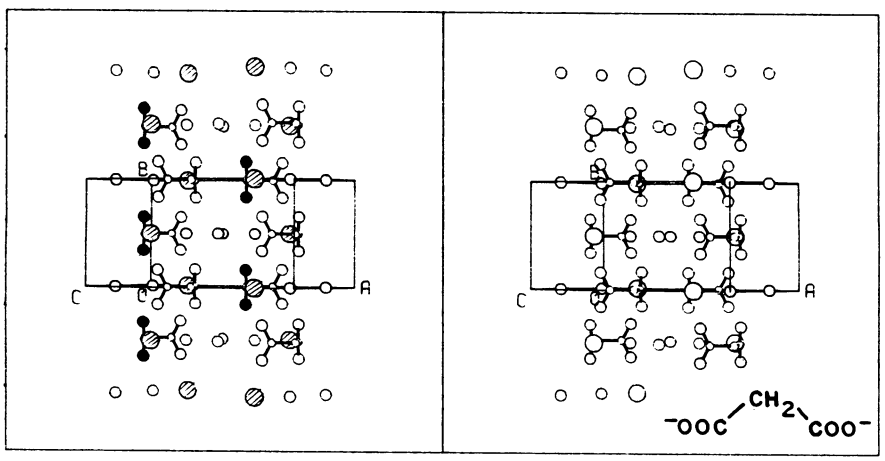


FIG. 2. Stereoscopic projection of the structure of calcium malonate dihydrate on the affected (101) face. The large circles represent calcium ions, the intermediate represent oxygens, and the small circles represent carbons. The shaded circles designate the carboxylate groups perpendicular to the face, and the hatched circles, the calcium ions with which they interact.

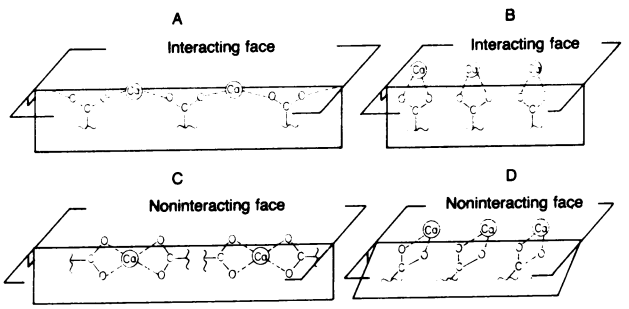


Scheme 2

the proteins shows that the carboxylate groups always emerge at some acute angle to the plane of the face (Scheme 2 *C* and *D*).

Both complexation motifs in the {101} and {10$\bar{1}$} faces define Ca–Ca and carboxylate–carboxylate repeating distances of 6.81 Å, which is matched by a repeating distance between alternate side chains along the protein polypeptide chain of a β-sheet (6.7–7.0 Å). This "match" of repeating distances is not sufficient, however, to explain the selectivity of the proteins for certain faces, as any face parallel to the *b* axis, or for that matter to the *c* axis, has a repeating Ca–Ca distance of 6.8 Å.

**Calcium Fumarate/- and Calcium Maleate/Aspartic Acid-Rich Protein Systems.** These were treated as described for the malonate system. They showed morphological changes that also indicate that specific interactions occurred. Examinations of the affected faces reveal the same features observed in the calcium malonate crystals with regard to the orientation of the emergent carboxylate groups (Fig. 3). Calcium tartrate, on the other hand, has no crystal planes with these characteristics and we observed no effect by the proteins, except at very high concentrations (equivalent to ≥5 μg of protein/ml). Under these conditions, a typical nonspecific binding effect is manifested by the formation of holes in the crystals, the presence of macroscopic steps, and by a general loss of well-defined crystal edges and shapes.

Calcium fumarate and maleate crystals were also grown in the presence of aspartate, glutamate, poly(aspartate), and poly(glutamate). These experiments (data not presented) showed that, whereas aspartate and glutamate have no effect on the growing crystals, poly(aspartate) in the β-sheet conformation has an effect very similar to that of the aspartic acid-rich matrix proteins. Polyglutamate, which mainly adopts a random-coil conformation, had only a weak, clearly nonspecific effect (unpublished results). We also tested the influence of the second class of matrix macromolecules, the serine-rich protein-polysaccharides, on growing calcium fumarate and maleate and found that they did not affect the morphologies of the crystals.

These experiments show that rigid, calcium-loaded aspartic acid-rich matrix proteins, which adopt the β-sheet conformation, can cooperatively bind only to those crystal faces in which the carboxylate groups are approximately perpendicular to the plane of the face (we call this the "stereochemical effect"). We attribute this effect primarily to the requirement of the protein-bound calcium ions to optimally complete their coordination polyhedrons with the carboxylate groups at the crystal surface. Ideally, this implies that carboxylates and calcium ions of the protein would occupy lattice sites of the substrate ions had the crystal layer been extended.

**Calcite/Aspartic Acid-Rich Protein System.** The structure of calcite (Fig. 4) is characterized by having alternate layers of calcium and carbonate ions along the *c* axis. The planar carbonate ions lie on the {001} plane (21). According to the stereochemical effect discussed above, the optimal plane for interaction between calcium-loaded aspartic acid-rich proteins and the growing crystal should be the {001} plane (Fig. 4), in which the planar carbonate ions are well aligned. Note that the best approach for a carboxylic group, with two binding oxygens, is in a perpendicular orientation to the calcium plane, whereas for a carbonate, with three binding oxygens, the best approach is parallel to the calcium plane.

Calcite crystals grown in the absence of protein develop the cleavage rhombohedral habit. Fig. 4 also shows the face of the cleavage rhombohedron [(100), according to the rhombohedral morphological nomenclature and (104) according to the hexagonal structure]. We found that growth of calcite is inhibited in a nonspecific manner (as in the case of calcium tartrate) at protein concentrations >0.5 μg/ml, thus confirming earlier observations (8). Crystals grown in the pres-

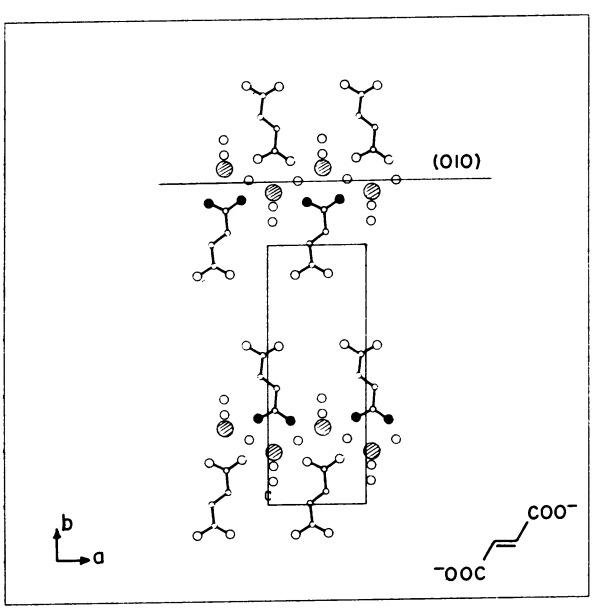


FIG. 3. Structure of calcium fumarate trihydrate viewed along the *c* axis with the affected (010) face viewed edge-on. The small shaded circles represent the carboxylate groups that emerge perpendicular to the face. The large hatched circles are the calcium ions involved in the complexation at the surface.

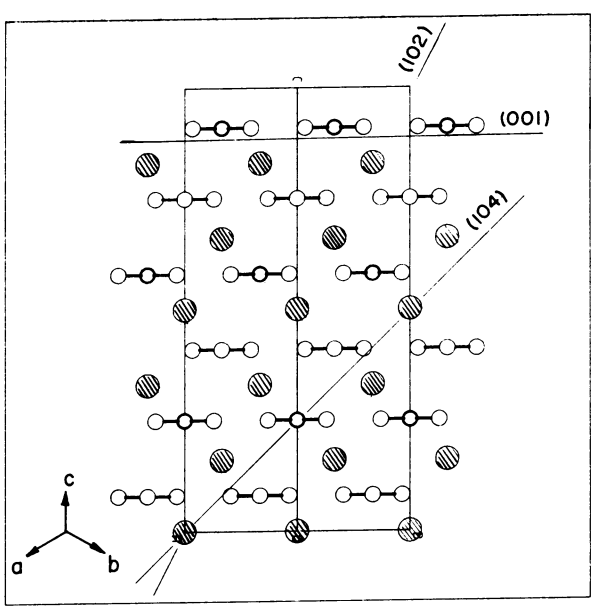


FIG. 4. Structure of calcite viewed perpendicular to the *c* axis.

ence of smaller amounts of protein still had rhombohedral morphology but, in addition, developed very small (001) faces (Fig. 5 *A* and *B*). Curiously, these (001) faces were located at only one of the cleavage rhombohedron vertices, even though the (001) and (00$\bar{1}$) faces are equivalent in the R$\bar{3}$c space group and should always behave symmetrically with respect to any external agent. This behavior is compatible with a process of nucleation in which the crystals grow out of the (001) plane. After nucleation, the crystal would form its normal rhombohedral morphology. Furthermore, we observed that the affected crystals were actually attached to the bottom of the glass vial, with the (001) face at the contact. We then grew calcite crystals in glass or plastic containers (Falcon cell culture dishes) that were previously incubated with protein solutions of various concentrations for 24 hr. After incubation, the vials were thoroughly washed and air-dried prior to the introduction of fresh supersaturated calcium carbonate solution. More than 50 different experiments, with protein and without protein, using different types of glass and plastic containers, often in the form of double-blind tests, showed that in the vials containing protein, 15–30% of the calcite crystals grew with the (001) face in contact with the container surface. In the absence of protein, only 1–3% of the crystals developed this face. Almost all the remaining crystals in these experiments had regular cleavage rhombohedral shapes and grew lying on their (104) face.

To verify that the acidic proteins were indeed in contact with the (001) face, we detached the crystals and incubated them with polyclonal antibodies, raised in rabbits, against the aspartic acid-rich proteins. We determined the presence or absence of bound antibody by indirect immunofluorescence. From 50 to 70% of the crystals showed fluorescence selectively on their (001) faces (Fig. 5*C*) in the presence of antibody, as compared to 0–5% when incubated with preimmune serum. To test for nonspecific binding of antibodies to the (001) face, we incubated crystals that had developed the (001) face in the absence of protein and found that <10% of them fluoresced on this face. Note that as the protein may remain adsorbed on the container surface when the crystals are detached, a higher yield of specifically fluorescing crystals is unlikely.

These experiments showed that calcite crystals developed one of their {001} faces as a result of being nucleated on acidic proteins that were previously adsorbed onto the container surface. The nucleating face is the one that the "stereochemical effect" predicts should develop.

## DISCUSSION

We have shown that the aspartic acid-rich mollusk shell matrix proteins interact specifically with certain faces of various calcium dicarboxylate crystals during their growth. The unique property of all the affected faces is that their carboxylate groups are oriented perpendicular to the face and can therefore optimally complete the coordination polyhedron around the protein-bound calcium ions (the stereochemical effect). The same proteins, once adsorbed on glass or plastic, act as nucleators of calcite specifically from the (001) hexagonal plane.

These observations highlight the importance of the aspartic acid-rich matrix proteins in crystal-growth regulation and emphasize the properties that enable a calcium-bound acidic protein in the $\beta$-sheet conformation to interact with a crystal surface—namely, the formation of a regular array of calcium and carboxylate ions which is available for cooperative binding to the crystal. The experiments show that although other factors (see below) may play a part in achieving the specific interaction, satisfying the stereochemical requirements is essential, at least in the systems we studied.

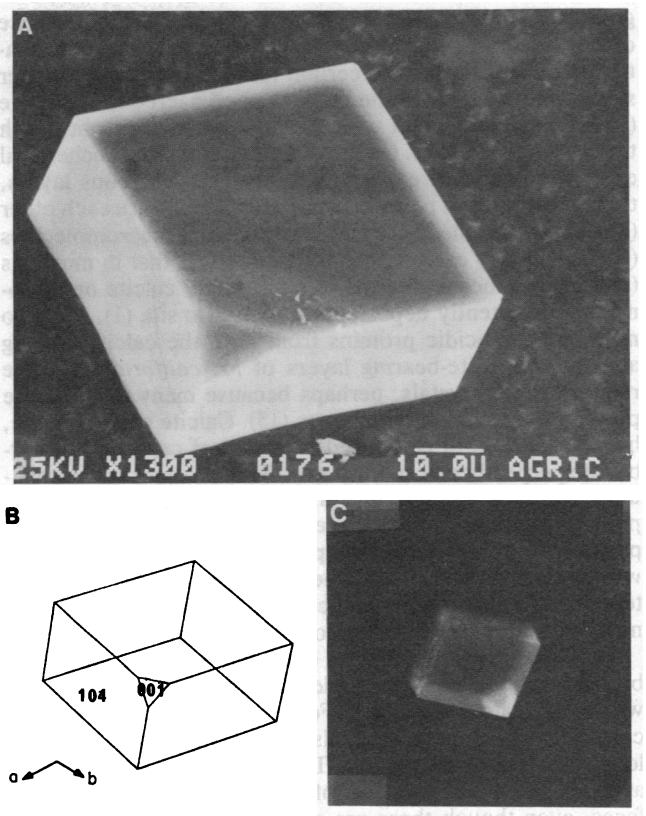


FIG. 5. (*A*) Scanning electron micrograph of a calcite crystal nucleated on acidic proteins adsorbed on the surface of a glass vial. The small triangular (001) face was attached to the vial surface. (×1000.) (*B*) Computer-drawn simulation of a calcite crystal in which one of the {001} faces is developed. (*C*) Indirect immunofluorescence staining of a calcite crystal, showing the presence of aspartic acid-rich protein on the {001} face.

Nonspecific interactions between charged surfaces cannot account for the morphological changes observed in the growth of calcium malonate, fumarate, and maleate. When this does occur, as with calcium tartrate crystals grown in the presence of high concentrations of protein, it can easily be distinguished from the specific type of interaction by the absence of well-developed crystal faces and edges. The observed interactions cannot be attributed only to a concentration of positive or negative charge density on the specific planes ("calcium planes"). In calcium malonate, for example, the face of highest calcium density, {100}, is the most developed in the pure crystals. Its disappearance in the affected crystals shows that this face does not preferentially interact with the proteins. In calcite there are at least two planes, (001) and (102), that are composed entirely of calcium (and, alternatively, of carbonate) ions (Fig. 4). The charged nature of the (001) face probably does favor the interaction with protein, but the fact that nucleation did not occur from (102), together with the information from the model compounds, suggests that charge density is not sufficient to account for the observed specificity. The possibility that specific interactions arise from ion spacing alone is also untenable, as many of the affected and the unaffected faces have the same Ca–Ca distances. We emphasize, however, that all the above factors may in part contribute to the interactions, but they alone cannot account for the observed specificity.

The large majority of biogenic calcite and aragonite crystals have their *c* axes oriented in a preferred direction, consistent with the importance that we attribute to the stereochemical effect in protein-modulated biological crystal

growth. Towe and Cifelli (22) also recognized the importance of this effect in contributing to the preferred *c*-axis orientation in calcite crystals of certain foraminifera. In the better studied cases, such as the mollusk shell nacreous layer, the (001) face is in contact with the matrix surface from which the crystals grow (23). On the other hand, the stereochemical effect alone cannot explain why, in some nacreous layers, the *a* and *b* axes of many crystals are aligned with each other (24) and with some of the juxtaposed matrix macromolecules (25, 26). It also cannot account for the fact that in mollusks (and many other organisms as well) either calcite or aragonite is consistently deposited at a specific site (1). We also note that the acidic proteins from both the calcite-bearing and the aragonite-bearing layers of *M. californianus* gave rise to calcite crystals, perhaps because many of the same proteins are found in both layers (15). Calcite and aragonite, however, are both composed of layers of calcium and carbonate perpendicular to the *c* axis. The locations of the calcium ions in the calcium layers are almost identical for both polymorphs. The major difference between the two is in the position of the carbonate groups. It is likely that under the *in vitro* conditions used here, the formation of a layer of protein-bound calcium ions induces the nucleation of the thermodynamically more stable polymorph calcite.

These results imply that an examination of the faces of a biogenic crystal could provide an indication of the site at which nucleation occurred. For example, in the prismatic calcite layers of mollusk shells, the *c* axis is parallel to the long axis of the prisms (23). The most likely site of nucleation is, therefore, the base of the prisms and not the side faces, even though these are also in close association with organic matrix. In the coccolith, *Emiliania huxleyi*, the lower elements of individual segments consist of calcite crystals in which the *c* axes are aligned with the morphological elongation of the structure (27, 28). The first incipient crystals are observed to form at both ends of the lower element (29) on planes perpendicular to the *c*-axis orientation corresponding to the (001) face. The eyes of some fossil trilobites contain calcite rhombohedrons that have their *c* axes oriented perpendicular to the visual surface (30, 31), suggesting that nucleation could have occurred on a protein substrate from the (001) face. The most developed face in tooth enamel hydroxyapatite crystals is the {100} face (16). Inspection of the molecular structure shows a linear repeating calcium-phosphate motif stereochemically equivalent to the calcium-carboxylate interaction shown in Scheme 2*B*, where the carboxylate is replaced by $^{O}\!\!\diagdown_{P}\!\!\diagup^{O}$.

Nucleation and inhibition of crystal growth have many common attributes. At the level of stereochemical control observed in the calcium carboxylate systems, on the one hand, and in calcite, on the other, specific nucleation and inhibition are in fact subject to very similar requirements. Nucleation, however, occurred when the proteins (or some of them) were adsorbed onto a rigid substrate, whereas inhibition occurred when the proteins in solution interacted with an already-formed crystal. This difference is apparently crucial in determining whether nucleation or inhibition will occur.

It is clear from these results, and in general from the existing knowledge on nucleation and inhibition, that both processes can be regulated at different levels, from the nonspecific to the very specific. In this context, we suggest that the two classes of matrix macromolecules examined, the aspartic acid-rich proteins and serine-rich protein–polysaccharide complexes, both present in mineralized tissues from widely divergent phyla (5), may perform different and possibly cooperative roles in crystal growth *in vivo*. The aspartic acid-rich proteins, after binding calcium, are capable of actively inducing, regulating, and inhibiting crystal growth *in vitro*. The serine-rich protein–polysaccharide complexes had, under our *in vitro* conditions, no noticeable effect on the growing crystals tested but presumably fulfill an important function *in vivo*.

In many organisms, crystal growth is mediated by acidic matrix constituents similar to those used in this study. Our series of *in vitro* experiments elucidate some of the basic principles by which these macromolecules interact in a specific manner with crystal surfaces. These same principles may also operate *in vivo*.

We thank F. Frolow for determining the structure of a new polymorph of calcium maleate; A. Lieberman, E. Shai, and T. Shuster for technical assistance; and Z. Berkovitch-Yellin, M. Lahav, L. Leiserowitz, H. A. Lowenstam, and W. Traub for useful discussions. Part of this work was supported by a U.S.-Israel Binational Science Foundation (BSF) grant (to S.W.) and by a Minerva Foundation (Munich) grant (to L.A.). L.A. is the recipient of the Helena Rubinstein Career Development Chair, and S.W. is the recipient of the Graham and Rhona Beck Career Development Chair.

1. Lowenstam, H. A. (1981) *Science* **211**, 1126.
2. Weiner, S., Traub, W. & Lowenstam, H. A. (1983) in *Biomineralization and Biological Metal Accumulation*, eds. Westbroek, P. & de Jong, E. W. (Reidel, Dordrecht, Holland), pp. 205–224.
3. Glimcher, M. J. (1981) in *The Chemistry and Biology of Mineralized Connective Tissues*, ed. Veis. A. (Elsevier, New York) pp. 617–673.
4. Veis, A. & Sabsay, B. (1983) in *Biomineralization and Biological Metal Accumulation*, eds. Westbroek, P. & de Jong, E. W. (Reidel, Dordrecht, Holland), pp. 273–284.
5. Weiner, S. (1984) *Amer. Zool.* **24**, 945–951.
6. Nawrot, C. F., Campbell, D. J., Schroeder, J. K. & Van Valkenburg, H. (1976) *Biochemistry* **15**, 3445–3449.
7. Termine, J. D., Eanes, E. D. & Conn, K. M. (1980) *Calcif. Tissue Int.* **31**, 247–251.
8. Wheeler, A. P., George, J. W. & Evans, C. A. (1981) *Science* **212**, 1397–1398.
9. Wilbur, K. M. & Bernhardt, A. M. (1984) *Biol. Bull.* **166**, 251–259.
10. Termine, J. D., Kleinman, H. K., Whitson, S. W., Conn, K. M., McGarvey, M. L. & Martin, G. R. (1981) *Cell* **26**, 99–105.
11. Watabe, N. & Wilbur, K. M. (1961) *J. Biophys. Biochem. Cytol.* **9**, 761–772.
12. Greenfield, E. W., Wilson, D. C. & Crenshaw, M. A. (1985) *Am. Zool.* **24**, 925–932.
13. Addadi, L., Berkovitch-Yellin, Z., Weissbuch, I., van Mil, J., Shimon, L., Lahav, M. & Leiserowitz, L. (1985) *Angew. Chem. Int. Ed. Eng.*, in press.
14. Addadi, L., Berkovitch-Yellin, Z., Domb, N., Gati, E., Lahav, M. & Leiserowitz, L. (1982) *Nature (London)* **296**, 21–27.
15. Weiner, S. (1983) *Biochemistry* **22**, 4139–4144.
16. Selvig, K. A. (1973) *Z. Zellforsch. Mikrosk. Anat.* **137**, 271–280.
17. Gupta, M. P., Prasad, S. M., Sahu, R. G. & Sahu, B. N. (1972) *Acta Crystallogr. Sect. B* **28**, 135–139.
18. Briggman, B. & Oskarsson, R. (1977) *Acta Crystallogr. Sect. B* **33**, 1900–1906.
19. Ambady, G. K. (1968) *Acta Crystallogr. Sect. B* **24**, 1548–1557.
20. Coppens, P., Leiserowitz, L. & Rabinovich, D. (1965) *Acta Crystallogr. Sect. B* **18**, 1035–1038.
21. Lippmann, F. (1973) in *Sedimentary Carbonate Minerals* (Springer, Berlin), pp. 6–16.
22. Towe, K. M. & Cifelli, R. (1967) *J. Paleontol.* **41**, 742–762.
23. Boggild, O. B. (1930) *K. Dan. Vidensk. Selsk. Skr. Naturvidensk. Math. Afd.* **2**, 231–326.
24. Wise, S. W. (1970) *Eclogae Geol. Helv.* **63**, 775–797.
25. Weiner, S. & Traub, W. (1980) *FEBS Lett.* **111**, 311–316.
26. Weiner, S., Talmon, Y. & Traub, W. (1983) *Int. J. Biol. Macromol.* **5**, 325–328.
27. Parker, S. B., Skarnulis, A. J., Westbroek, P. & Williams, R. J. P. (1983) *Proc. R. Soc. London Ser. B* **219**, 111–117.
28. Watabe, N. (1967) *Calcif. Tissue Res.* **1**, 114–121.
29. Wilbur, K. M. & Watabe, N. (1963) *Ann. N.Y. Acad. Sci.* **109**, 82–112.
30. Towe, K. M. (1973) *Science* **179**, 1007–1009.
31. Clarkson, E. N. K. & Levi-Setti, R. (1975) *Nature (London)* **254**, 663–667.